

Zirconium(IV) and hafnium(IV) coordination polymers with a tetra-acetyl-ethane (Bisacac) ligand: Synthesis, structure elucidation and gas sorption behavior

Felix Hentschel^a, Vladimir V. Vinogradov^b, Alexandr V. Vinogradov^b, Alexander V. Agafonov^c, Vadim V. Guliants^d, Ingmar Persson^a, Gulaim A. Seisenbaeva^a, Vadim G. Kessler^{a,*}

^a Department of Chemistry, BioCenter, Swedish University of Agricultural Sciences, Box 7015, 75007 Uppsala, Sweden

^b ITMO University, Kronverkskiy pr, 49, St. Petersburg 197101, Russia

^c Institute of Solution Chemistry, Russian Academy of Sciences, ul. Akademicheskaya 1, Ivanovo 153045, Russia

^d Department of Chemical, Environmental and Materials Engineering, University of Cincinnati, Cincinnati, OH 45221-0012, USA

ARTICLE INFO

Article history:

Received 4 October 2014

Accepted 19 December 2014

Available online 30 January 2015

Keywords:

Coordination polymer

Zr

Hf

Beta-diketonate

Gas sorption

ABSTRACT

Octahedrally shaped crystals of $\text{Zr}(\text{Bisacac})_2$ and $\text{Hf}(\text{Bisacac})_2$, M(IV) derivatives of bis-acetylacetone (tetra-acetyl-ethane), $\text{H}_2\text{Bisacac}$, were obtained in quantitative yield by a simple and reproducible synthetic procedure. The coordination spheres of Zr and Hf were found to be very closely related to those in molecular beta-diketonates, $\text{M}(\text{acac})_4$, according to the data of EXAFS spectroscopy. The structures are highly disordered, reflecting the multitude of conformations possible for each M(IV) centre. Crystal structure models involving metal centres with tetrahedrally arranged binding nodes were proposed for $\text{M}(\text{Bisacac})_2$. The produced materials are microporous with pronounced temperature-dependent affinity and selectivity to hydrogen gas absorption.

© 2015 Elsevier Ltd. All rights reserved.

1. Introduction

Three-dimensional coordination polymers, poorly soluble salts of bi- or polydentate anions, can form porous structures, often referred to today as Metal–Organic Frameworks (MOFs) [1]. They have in recent years gained increasing attention due to a plethora of attractive applications within catalysis [2], optical sensing and bioimaging [3], gas storage [4] and last, but not least, gas separation [5]. A common approach to the synthesis of MOFs has been focused on aqueous conditions and the use of ligands such as bis- and polycarboxylates as nodes, complemented mostly by 3d transition metals with bis- and polyamine moieties [2,6]. The use of highly charged 4d and 5d cations potentially opens access to MOFs with improved thermal and chemical stability. This explains the attention attracted by the discovery of the $\text{Zr}_6\text{O}_4(\text{OH})_4\text{L}_{12}$ octahedral building block (where L is a carboxylate residue), of which the terephthalate derivative UiO-66 is the first representative of the MOF family [7]. Its members responded well to the set expectations and demonstrated well developed mesoporosity together with high surface areas with an order of magnitude of

850–1300 m^2/g by N_2 adsorption [7] and, in the case of the terephthalate derivatives, also facile functionalization of the core with the prospect of applications in catalysis [8]. The synthesis of materials from the UiO-66 family could no longer be successfully achieved in aqueous medium because of the competition with hydrolysis of the M(IV) cations. Instead polar organic solvents, such as DMF, together with solvothermal conditions and the use of the highly moisture-sensitive anhydrous chloride, ZrCl_4 , as a starting reagent were required for their preparation. Compounds of the UiO-66 series belong to orthogonal crystal structures of the type I^0O^3 , according to the classification proposed by Cheetham et al. [9], where the pores are well-ordered and aligned. This structure type definitely has many advantages for application in catalysis, while for gas separation a complex pore geometry offered by a zeolitic network may appear more advantageous.

An alternative to carboxylate bridging anions in the construction of coordination polymers can potentially be bis-beta-diketonate ligands, where two beta-diketonate functions are joined by a carbon chain fragment (see Fig. 1). However, only a few bis-beta-diketonates are known in the literature. Problems in their synthesis are often found in the complex chemical reactivity of the ligand that can potentially lead to the formation of side products. Known representatives of this class of complexes are limited to derivatives of late 3d transition elements. They feature an

* Corresponding author.

E-mail address: vadim.kessler@slu.se (V.G. Kessler).

URL: <http://www.slu.se/en/departments/chemistry-biotechnology/>

octahedral geometry of the metal centers. The resulting polymers, dependent on additional ligands, are either one- or two-dimensional structures [10].

Bis-beta-diketonate complexes of Zr or Hf have not, to the best of our knowledge, been reported so far. Complexes of M^{4+} cations with common β -diketonate ligands, such as acetyl-acetonate (acac) or 2,3,6,6-tetramethyl-heptanedione (thd), are relatively poorly soluble and quite chemically and thermally stable materials, which appeared as a promising starting point in the search for approaches to their coordination polymer analogs with bis-beta-diketonate ligands.

In our earlier studies on the structures of Zr and Hf beta-diketonates, $M(\beta\text{-diketonate})_4$, it was found that molecules of these complexes possessed a pseudo tetrahedral topology. The coordination geometry of the central atoms comprising the oxygen donor atoms is an antiprism (see Fig. 2) [11]. Crystal structures of these compounds resulted from dense cubic packing of the molecules that acted as spheroids. Their pseudo tetrahedral topology resulted only in a lowered symmetry of the structure.

We hypothesized that the use of bis-beta-diketonate ligands will join the tetrahedral centers and result in their connection into a coordination polymer framework.

2. Experimental

All operations with metal–organic precursors were carried out in a dry nitrogen atmosphere using Schlenk line or a dry box techniques. The solvents toluene, hexane, n-propanol and iso-propanol were obtained from Aldrich and dried using conventional techniques. The precursors, dry crystalline $[Zr(O^iPr)_4(^iPrOH)]_2$ and $[Hf(O^iPr)_4(^iPrOH)]_2$, and a 70 wt% solution of $Zr(O^iPr)_4$ in iPrOH were purchased from Aldrich and used as received.

2.1. Synthetic procedures

In a typical synthetic procedure, about 0.5 g of the corresponding zirconium or hafnium alkoxides were dissolved in 5 ml toluene, then 2 eq of $H_2Bisacac$ were added together with an additional 2 ml toluene, and the mixture was subjected to reflux for 10 min. The white powder that formed was left for sedimentation over 2 days or, alternatively, precipitated by centrifugation, separated by decantation, washed twice with 5 ml warm anhydrous EtOH (Solveco) and dried in air.

Model samples of $M(acac)_4$ were obtained adding 4 eq of Hacac to solutions of ca 0.5 g of $[M(O^iPr)_4(^iPrOH)]_2$, $M = Zr, Hf$ in 5 ml toluene. The needle shaped crystals that formed were separated by decantation, washed with minimal amounts of dry hexane and dried in vacuum.

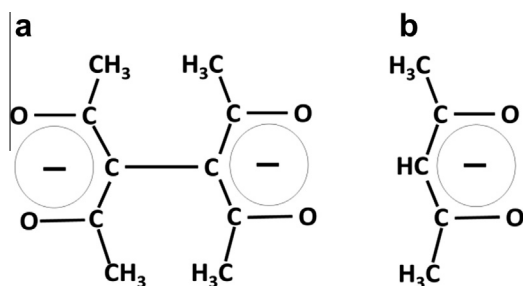


Fig. 1. Schematic representation of (a) the bis-beta-diketonate ligand (tetra-acetyl-ethane, $Bisacac^{2-}$) and (b) the related common beta-diketonate ligand (acetylacetone, $acac^-$).

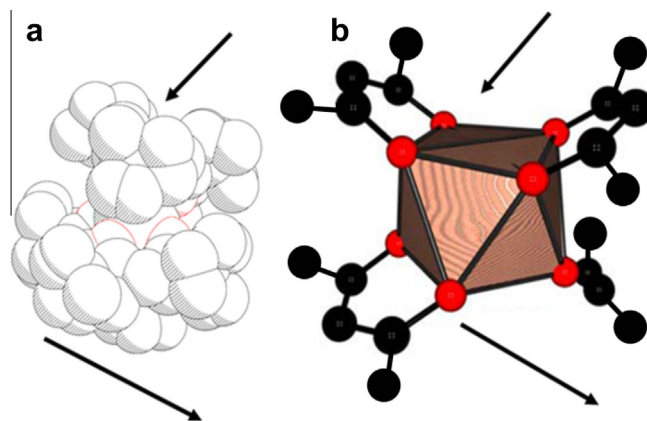


Fig. 2. Pseudo tetrahedral topology of the $M(\beta\text{-diketonate})_4$ molecules: the space-filling view (a) and one of the conformations of the core geometry (b) of the $M(thd)_4$ complexes, $M = Zr, Hf$ [11]. The arrows indicate orthogonal vectors of the tetrahedron.

2.2. Characterization

SEM-EDS studies were carried out with a Hitachi TM-1000- μ -DeX tabletop scanning electron microscope. TEM investigations were made using a Philips TECNAI G2 F20 transmission electron microscope (Roanoke, VA, USA) with an accelerating voltage of 200 kV. X-ray powder patterns were obtained using a Bruker SMART Apex-II diffractometer operating with Mo $K\alpha$ radiation ($\lambda = 0.71073 \text{ \AA}$). BRUKER APEX-II and EVA software were used for integration and data treatment. For determination of the adsorption capacity and textural characteristics (active surface area, pore volume and average pore size) ca 50 mg samples of compound **1** were used. The N_2 adsorption–desorption isotherms were measured at 77 K using a Micromeritics TriStar 3000 porosimeter. The hydrogen adsorption was performed on a Micromeritics ASAP2020 instrument at 77 and 293 K. The samples were first evacuated for 30 min at room temperature prior to the measurements. Thermal characteristics of the prepared powders and the adsorption properties of evacuated samples were studied using a Perkin-Elmer Pyris-1 TGA instrument connected for gas analysis with a Perkin-Elmer Spectrum 100 FTIR instrument. The latter was also used for recording the FTIR spectra of the samples in the form of KBr tablets.

2.3. Crystallography

Single crystals of the model complexes $Zr(acac)_4$ and $Hf(acac)_4$ were collected from a dispersion in Nujol oil and sealed in Lindeman tubes for X-ray experiments. The data collection was carried out at room temperature using a SMART Apex-II instrument operating with Mo $K\alpha$ radiation ($\lambda = 0.71073 \text{ \AA}$). BRUKER APEX-II software was used for integration and data treatment. The structures were solved by direct methods. The coordinates of all non-hydrogen atoms were located from the initial solution and refined first in an isotropic and then in an anisotropic approximation. The hydrogen atoms were all located in the difference Fourier syntheses and included in the final refinement steps in an isotropic approximation. For details of data collection and refinement please see [Electronic supplementary data](#).

2.4. EXAFS spectroscopy

Zirconium K and hafnium L_{III} edge X-ray absorption spectra were recorded at the wiggler beam line I811 at the MAX-Lab, Lund University, Lund, Sweden. The facility operated at 1.5 GeV and a

maximum current of 250 mA. The EXAFS station was equipped with a Si [111] double crystal monochromator. The solids, diluted and carefully ground with boron nitride, were contained in 1.0 mm aluminum frames covered with X-ray transparent tape. The experiments were performed in the transmission mode using gas filled ion chambers. Higher order harmonics were discarded by detuning the second monochromator crystal to 60% for hafnium and 80% for zirconium of maximum intensity at the end of the scans. The energy scale of the X-ray absorption spectra was calibrated by assigning the first inflection point of the K edge of a zirconium foil to 17997 eV and the L_{III} edge of a hafnium foil to 9555 eV [16]. The EXAFSPAK program package [17] was used for the data treatment. *Ab initio* calculated phase and amplitude parameters, used by the EXAFSPAK program, were computed by the FEFF7 program [18]. The standard deviations reported for the refined parameters were obtained from k^3 weighted least squares refinements of the EXAFS function (k), and do not include systematic errors. These statistical error values allowed reasonable comparisons, e.g. the significance of the relative shifts in the distances. However, the variations in the refined parameters, including the shift in the E_0 value (with $k = 0$), using different models and data ranges, indicated that the absolute accuracy of the distances is within 0.005 to 0.02 Å for well-defined interactions. The “standard deviations” have been increased accordingly to include estimated additional systematic errors.

3. Results and discussion

In the present work we used the commercially available bis-acetylacetone, $H_2Bisacac$ (tetraacetyl ethane, $(CH_3CO)_2CH-CH(COCH_3)_2$, CAS No. 5027-32-7) as the simplest representative of the bis-beta-diketonate family of ligands. The reaction between soluble zirconium or hafnium alkoxides and 2 eq. of the ligand produced quantitatively octahedrally shaped crystals (see Fig. 3) that could be purified from a possible excess of the ligand by extraction of the latter with $iPrOH$ on reflux or by its sublimation in vacuum. The mother liquor was then free from metal content, indicating the completeness of the transformation. The synthetic procedure was very facile, quick and reproducible, opening access to large-scale synthesis of this material, which is insoluble in organic solvents and, containing 2 bis-beta-diketonate ligands per metal center, is apparently a coordination polymer.

To probe the molecular structure of the obtained compound and to determine the coordination geometry and the distances from the central metal atom to surrounding atoms in the obtained structures, EXAFS (extended X-ray absorption fine structure)

spectroscopy was applied. The data quality was sufficient to determine the M–O and M...C distances and the three-leg M–O–C and MO_8 core multiple scattering with good accuracy. The number of distances was kept fixed at the expected value as the correlation between the number of distances and Debye–Waller coefficients is strong. The results of the refinements of the distances and Debye–Waller coefficients are summarized in Table 1, and the fitting of the raw data as well as the Fourier transforms are shown in Figs. 4 and 5. The obtained structural parameters for the solid

Table 1

EXAFS data: mean bond distances, $d/\text{Å}$, number of distances, N , Debye–Waller coefficients, $\sigma^2/\text{Å}^2$, amplitude reduction factors, S_0^2 , threshold energies, E°/eV , and the goodness of fit as defined in the EXAFSPAK program, $F/\%$, in the refinements of solid zirconium(IV) and hafnium(IV) acetylacetonate and bis-acetylacetonate at room temperature. The refinements were performed in the k range 2–13 Å^{-1} .

Interaction	N	d	σ^2	S_0^2	E°	F
<i>Solid zirconium(IV) acetylacetonate</i>						
Zr–O	8	2.193(1)	0.0054(1)	1.01(1)	18018.0	8.9
Zr...C	8	3.168(2)	0.0068(2)			
Zr...C	16	3.306(4)	0.0068(2)			
Zr...C	8	3.577(4)	0.0073(2)			
Zr...C	16	4.488(8)	0.0092(2)			
MS (ZrO_8)	16+8+16	4.40(1)	0.010(2)			
<i>Solid zirconium(IV) bisacetylacetonate</i>						
Zr–O	8	2.160(1)	0.0052(1)	0.91(1)	18017.0	9.8
Zr...C	8	3.196(2)	0.0068(1)			
Zr...C	16	3.309(4)	0.0067(2)			
Zr...C	8	3.62(1)	0.0073(2)			
Zr...C	16	4.48(1)	0.010(1)			
MS (ZrO_8)	16+8+16	4.33(1)	0.011(2)			
<i>Solid hafnium(IV) acetylacetonate</i>						
Hf–O	8	2.180(1)	0.0048(1)	0.82(1)	9584.5	12.6
Hf...C	8	3.182(2)	0.0061(2)			
Hf...C	16	3.310(4)	0.0067(2)			
Hf...C	8	3.59(1)	0.0073(2)			
Hf...C	16	4.485(4)	0.012(1)			
MS (HfO_8)	16+8+16	4.37(1)	0.010(2)			
<i>Solid hafnium(IV) bisacetylacetonate</i>						
Hf–O	8	2.150(1)	0.0046(1)	0.66(1)	9584.3	15.7
Hf...C	8	3.195(7)	0.0088(2)			
Hf...C	16	3.303(4)	0.0097(3)			
Hf...C	8	3.634(8)	0.0108(2)			
Hf...C	16	4.49(1)	0.013(1)			
MS (HfO_8)	16+8+16	4.41(3)	0.009(2)			

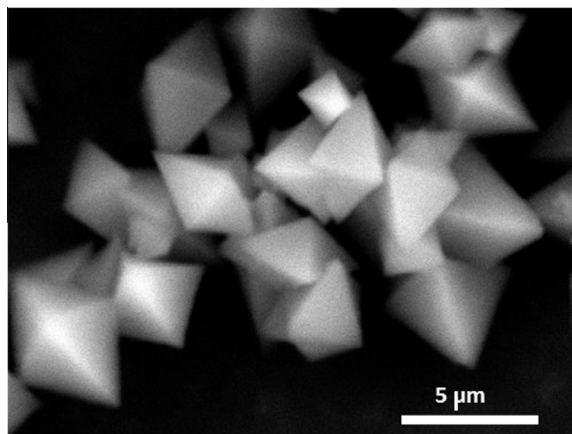


Fig. 3. SEM image of the $Zr(Bisacac)_2$ crystals.

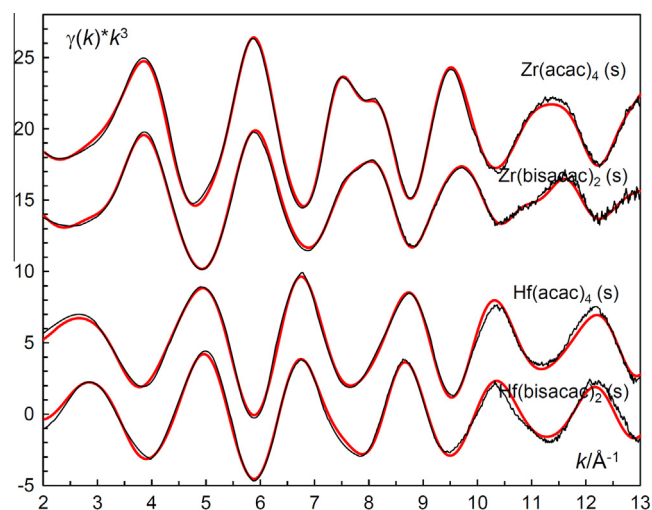


Fig. 4. k^3 weighted EXAFS of solid (a) $Zr(acac)_4$, (b) $Zr(Bisacac)_2$, (c) $Hf(acac)_4$ and (d) $Hf(Bisacac)_2$ with offset of 20, 15, 5 and 0, respectively; experiment (thin black line); model (red line). (Color online.)

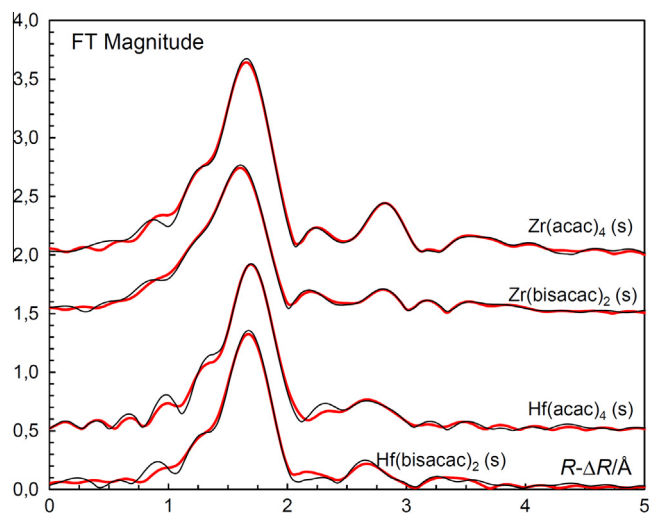


Fig. 5. Fourier transform of the k^3 weighted EXAFS function of solid (a) $\text{Zr}(\text{acac})_4$, (b) $\text{Zr}(\text{bisacac})_2$, (c) $\text{Hf}(\text{acac})_4$ and (d) $\text{Hf}(\text{bisacac})_2$ with offset of 2.0, 1.5, 0.5 and 0, respectively; experiment (thin black line); model (red line). (Color online.)

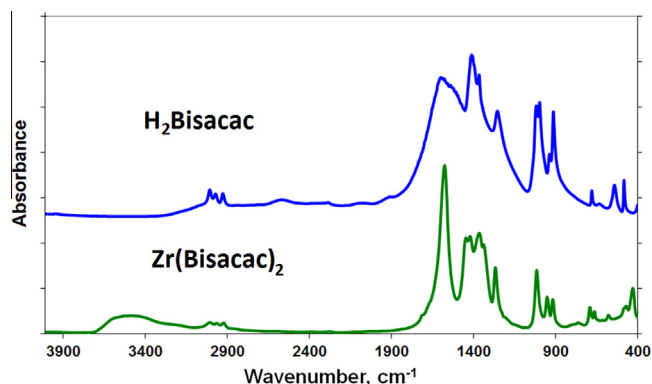


Fig. 6. FTIR spectrum of the $\text{Zr}(\text{bisacac})_2$ complex in comparison with that for the free $\text{H}_2\text{Bisacac}$ ligand.

zirconium(IV) and hafnium(IV) acetylacetonate complexes are in very good agreement with the data obtained by single crystal experiments in this and previous studies (see Fig. 2 and FS1) [12]. The M–O bond distances in the bis-acetylacetonate

complexes are significantly shorter, ca. 0.03 Å, than in the corresponding acetylacetonate ones, Table 1. Furthermore, the M–O–C bond angle in the bisacetylacetonate complexes is significantly larger, by ca. 5°, with mean angles of 131°, 133°, 136° and 137° in $\text{Zr}(\text{acac})_4$, $\text{Hf}(\text{acac})_4$, $\text{Zr}(\text{bisacac})_2$ and $\text{Hf}(\text{bisacac})_2$, respectively. These differences in the M–O bond lengths and values of the M–O–C bond angles between the bisacetylacetonate [10] and acetylacetonate [13] complexes are typically observed for a broad series of derivatives of transition elements (Co, Cu, Zn, Ru, etc.). The M...C distances to the methylene and terminal carbons are ca. 3.6 and 4.5 Å, respectively.

It is important to stress that the close resemblance between the EXAFS spectra of different compounds is a direct indication of analogous coordination geometries of the studied centers in them. This resemblance is clearly manifested in Figs. 4 and 5.

The results of the EXAFS study prove unambiguously that the first and second coordination spheres in the produced coordination polymers have constructions truly closely resembling those of the molecular $\text{M}(\text{acac})_4$ complexes. The first coordination sphere features definitely an Archimedes antiprism configuration of the MO_8 core. The second coordination sphere is composed of the carbon atoms of the ligands.

Strong bonding interactions between the M(IV) cations and the ligand can easily be traced in the FTIR spectra (Fig. 6) that are noticeably different from those of the free tetra-acetyl-ethane ligand. All the regions of the spectra display shifting and most likely also a considerable symmetry change. The triplet in the C–H stretching area is located at 3013, 3000 and 2935 cm^{-1} in the free ligand and at 3000, 2997 and 2950 cm^{-1} in the MOF. Broad bands at 1613 and 1564 cm^{-1} arising from C=O stretching in the spectrum of the free ligand are replaced by a single band at 1580 cm^{-1} in the complex, indicating that it is present in a symmetric conjugated form. The C–C stretching region, between 1100 and 900 cm^{-1} , also undergoes a clear simplification (a reduction from 4 to 3 bands), apparently as a result of the transformation from an asymmetric enol form in the free ligand to a symmetric conjugated anion in the complex.

A relatively intensive band at 439 cm^{-1} apparently originates from Zr–O vibrations in the spectrum of the complex. It is interesting to note that the MOF stored at an ambient atmosphere is apparently adsorbing water, as indicated by the characteristic stretching and bending O–H modes at 3550 and 1723 cm^{-1} respectively that emerge in its FTIR spectrum. The reversible adsorption of water has been unequivocally confirmed by TGA-FTIR experiments (see Fig. 7). The first step in the TGA curve

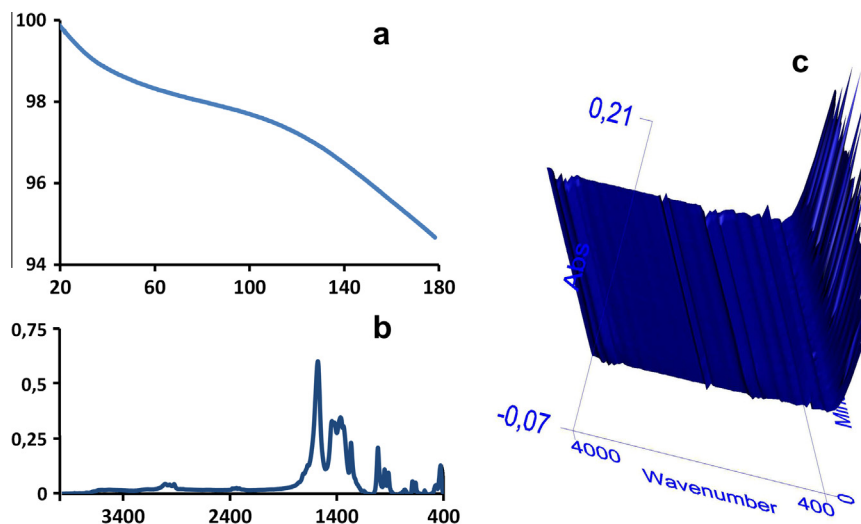


Fig. 7. The TGA curve for heating of **1** in air in the 20–180 °C interval (a), FTIR spectrum of the solid residue (b) and the FTIR spectrum of the outgoing gases (c).

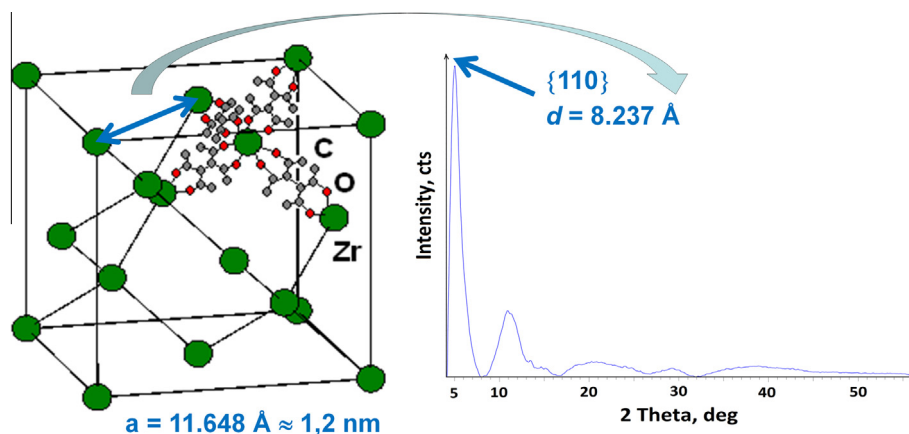


Fig. 8. The structure model for the $\text{Zr}(\text{Bisacac})_2$ material and its X-ray powder pattern with a highlighted characteristic diffraction peak.

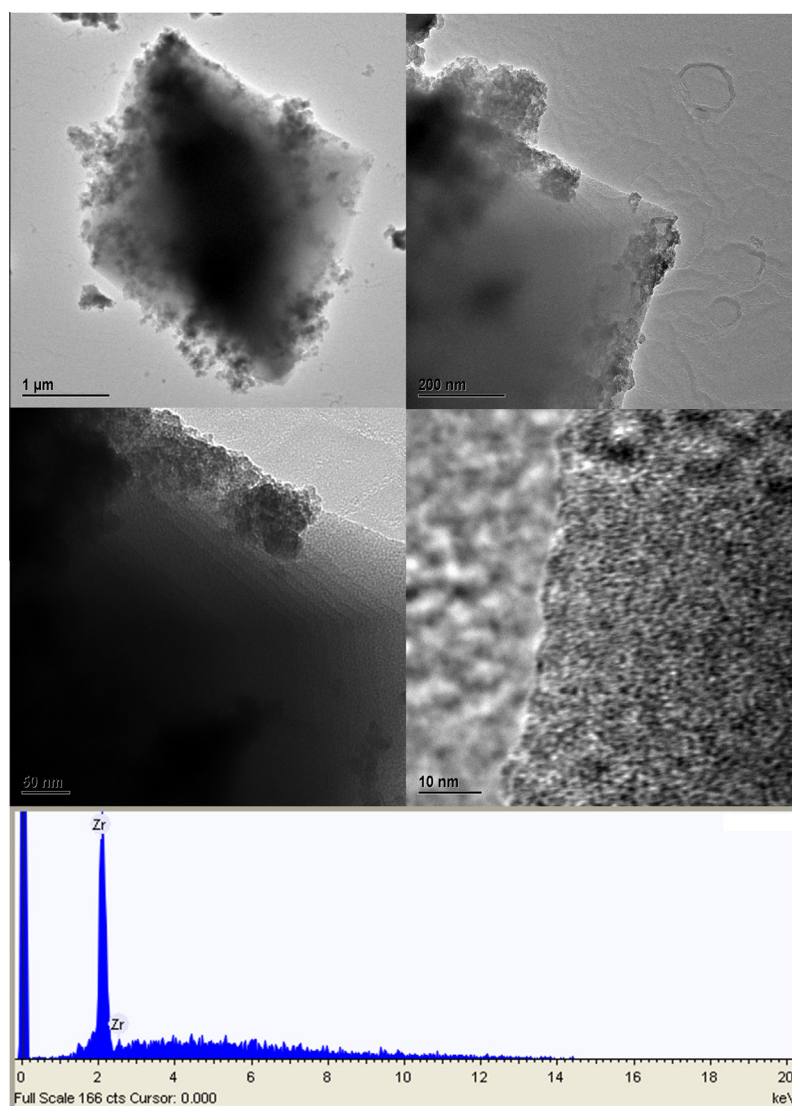


Fig. 9. TEM views and a representative EDS spectrum of the $\text{Zr}(\text{Bisacac})_2$ compound.

in the 20–180 °C temperature interval is associated very clearly with the release of water vapor, as indicated by the FTIR spectra of the outgoing gases. The spectrum of the residual solid is indistinguishable from that of the initial compounds **1** and **2**, but is practically lacking the peaks corresponding to the O–H vibrations.

In striking contrast to the well-ordered setup of the coordination spheres of the metal atoms, the structures of the $\text{M}(\text{Bisacac})_2$ ($\text{M} = \text{Zr}$ and Hf) polymers, closely analogous to each other, appear to lack the long-range order almost completely. Their powder diffraction patterns (Fig. 8 and FS2) feature a few extremely broad

lines, indicating extant disorder and small diffraction correlation domains. The first peaks observed in the patterns are relatively better defined and correspond apparently to the dominating interlayer distance coinciding with the metal–metal distance in the $M(\text{CH}_3\text{CO})_2\text{C}-\text{C}(\text{COCH}_3)_2M$ fragments at 8.273 Å for Zr and 8.586 Å for Hf.

These distances correlate very well with the M–M distances in the $M(\text{CH}_3\text{CO})_2\text{C}-\text{C}(\text{COCH}_3)_2M$ fragments observed in the 3d transition metal complexes of this ligand [10]. It can be hypothesized that the latter is half of the face diagonal of the zeolite- or “diamond”-like face centered cubic lattice, which had logically to emerge from the attachment of the applied tetrahedral centers to each other via linear ligand nodes. The Miller index $\{hkl\}$ for such a fragment would be $\{110\}$. The unit cell parameter a can thus be obtained as $a = d_{110} \cdot \sqrt{2} = 11.648$ Å (for $M = \text{Zr}$). Possible indexing of the other less well defined peaks in the pattern is in agreement with the proposed structural model.

The obtained X-ray patterns are quite peculiar. The unit cells are relatively small and presumably highly symmetric (cubic), but apparently only short-order contacts are sufficiently well defined in the structure. This can be understood taking into account the disorder otherwise present in the molecular analogs of the produced coordination polymers. Also in the structures of $M(\text{thd})_4$, $M = \text{Zr, Hf}$, there were 3 different isomers of molecules observed, originating from 3 different mutual orientations of the ligands possible for just one metal oxygen core [11]. In the molecular structures the distribution of different configurations was statistical and could be rationalized via single crystal experiments as components in the observed positional disorder for the carbon atoms. In the 3D polymer structure one can easily imagine that the disorder should be resolved locally and physically at short distances as the centers are attached to each other. However, for the longer range, beyond one unit cell, one can expect that a center or block of centers with one conformation gets attached to center or block with a different conformation. This means that these materials belong to the family of pseudo crystalline substances,

such as, for example, DNA, usually displaying only one rather broad strong reflection at a low theta angle and elusive weak and even broader ones at higher angles [14].

The consequence of the observed pseudo crystalline nature of the obtained materials would be the emergence of irregular wormhole porosity in their structures that, remaining crystalline with respect to positioning of the metal centers, are in reality amorphous as a consequence of irregularities in the positioning of the carbon atoms. This dual behavior can in fact be traced via TEM studies of the produced materials, as well as in SEM where it is possible to observe octahedral crystals with sharp and regular edges (Fig. 9). Even the regular planar dislocations reflecting the growth of the crystals can clearly be distinguished on the faces of the octahedrons. The high resolution images, however, fail completely to reveal any long-range ordered structure. Instead, a pattern of wormhole porosity with intermitting denser and lighter domains close in size to about 1.2 nm (a single unit cell) are revealed. This observation is in full agreement with the prediction made above.

The complex micropore geometry in combination with the high density of non-polar methyl groups permitted the supposition that the produced materials might exhibit interesting characteristics with respect to gas, and in particular hydrogen, sorption. In fact the investigated Zr-based coordination polymer exhibited a relatively low pore volume as determined by nitrogen sorption ($0.09 \text{ cm}^3/\text{g}$) and quite a limited surface area of $260 \text{ m}^2/\text{g}$, where $195 \text{ m}^2/\text{g}$ are caused by micropores. Taking into account the quite small size of the crystals themselves (1–5 μm), it can be concluded that the crystals possess intrinsically only microporosity, while the total area reflects even adsorption on the surface of the (quite small) crystals.

An interesting feature of this material is its strongly temperature-dependent hydrogen adsorption. At room temperature it practically does not adsorb hydrogen at all (0.033 mmol/g at 1 atm), while at 77 K it displays considerable absorption (1.80 mmol/g at 1 atm). This difference arises apparently from the temperature induced “swelling” of the structure. On cooling it undergoes relaxation and becomes more ordered, most probably with unification of the conformations for the metal centers and both opening and improved accessibility of the pores.

On warming to room temperature a complex equilibrium of different conformations results in entangling and closing of the pores, which may even become effectively smaller because of the vibrations in the structure (Fig. 10), and hydrogen adsorption decreases practically to zero. The materials revealed no apparent mesoporosity, resulting in isotherms lacking hysteresis. That is why only the adsorption parts are displayed in the Fig. 10. The materials are relatively thermally stable and decompose at temperatures over 260°C (for samples not subjected to deeper purification). The observed hydrogen uptake is not strikingly high, 0.36 wt% compared to 2.9 wt% for the MOFs based on 3d-transition elements and aromatic di-carboxylate ligands, but can supposedly be improved if bigger bis-beta-diketonate spacers are used – a detailed discussion of factors influencing the efficiency of hydrogen adsorption and an overview of related materials can be found in a recent review [15].

4. Conclusions

Pseudocrystalline coordination polymer complexes of Zr(IV) and Hf(IV) cations with the tetra-acetyl-ethane (Bisacac) ligand have been successfully produced in high yields by the reaction of the alkoxides of these elements with stoichiometric amounts of the ligand. The molecular structures of the produced materials are closely related to those of the molecular beta-diketonate models, as demonstrated by EXAFS spectroscopy. Their highly disordered crystal

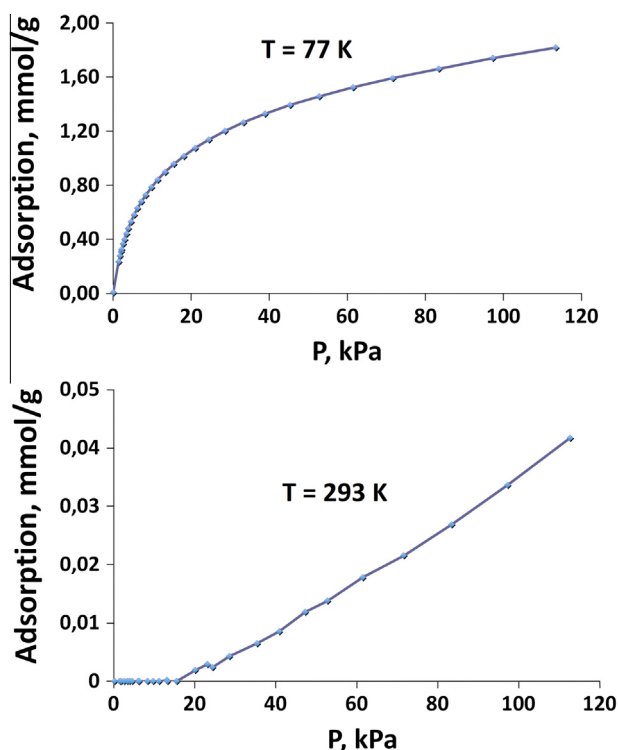


Fig. 10. Hydrogen adsorption isotherms for the $\text{Zr}(\text{Bisacac})_2$ compound at 77 and 293 K.

structures, formed by the coupling of tetrahedral centers, are most probably following a simple “diamond” type (face-centered cubic) motif. The obtained coordination polymers display a strong temperature dependence in relation to hydrogen absorption, facilitated supposedly by their pseudo crystalline nature.

Acknowledgments

This work was supported by grants from Swedish Research Council (Molecular precursors and molecular models of nanoporous materials), EU Leonardo program and the Ministry of Higher Education of Russian Federation (aimed at maximizing the customer's competitive advantage among world leading educational centers).

Appendix A. Supplementary data

CCDC 980277 and 980278 contain the supplementary crystallographic data for Zr(acac)₄ and Hf(acac)₄, respectively. These data can be obtained free of charge via <http://www.ccdc.cam.ac.uk/conts/retrieving.html>, or from the Cambridge Crystallographic Data Centre, 12 Union Road, Cambridge CB2 1EZ, UK; fax: (+44) 1223-336-033; or e-mail: deposit@ccdc.cam.ac.uk. Supplementary data associated with this article can be found, in the online version, at <http://dx.doi.org/10.1016/j.poly.2014.12.041>.

References

- [1] (a) H.C. Zhou, J.R. Long, O.M. Yaghi, *Chem. Rev.* 112 (2012) 673; (b) M. O'Keeffe, O.M. Yaghi, *Chem. Rev.* 112 (2012) 675.
- [2] (a) L. Ma, C. Abney, W. Lin, *Chem. Soc. Rev.* 38 (2009) 1248; (b) D. Farrusseng, S. Aguado, C. Pinel, *Angew. Chem., Int. Ed.* 48 (2009) 7502; (c) J.Y. Lee, O.K. Farha, J. Roberts, K.A. Scheidt, S.B.T. Nguyen, J.T. Hupp, *Chem. Soc. Rev.* 38 (2009) 1450; (d) A. Corma, H. Garcia, F.X. Llabres i Xamena, *Chem. Rev.* 110 (2010) 4606; (e) M. Yoon, R. Srirambalaji, K. Kim, *Chem. Rev.* 112 (2012) 1196.
- [3] (a) K.M.L. Taylor, W.J. Rieter, W. Lin, *J. Am. Chem. Soc.* 130 (2008) 14358; (b) K.M.L. Taylor, A. Jin, W. Lin, *Angew. Chem., Int. Ed.* 47 (2009) 7722; (c) K.E. deKrafft, Z. Xie, G. Cao, S. Tran, L. Ma, O.Z. Zhou, W. Lin, *Angew. Chem., Int. Ed.* 48 (2009) 9901; (d) L.E. Kreno, K. Leong, O.K. Farha, M. Allendorf, R.P. Van Duyne, J.T. Hupp, *Chem. Rev.* 112 (2012) 1105.
- [4] (a) A. Phan, C.J. Doonan, F.J. Uribe-Romo, C.B. Knobler, M. O'Keeffe, O.M. Yaghi, *Acc. Chem. Res.* 43 (2010) 58; (b) S.S. Han, J.L. Mendoza-Cortés, W.A. Goddard, *Chem. Soc. Rev.* 38 (2009) 1460; (c) D.Q. Yuan, D. Zhao, D. Sun, H.C. Zhou, *Angew. Chem., Int. Ed.* 49 (2010) 5357.
- [5] (a) J.R. Li, R.J. Kuppler, H.C. Zhou, *Chem. Soc. Rev.* 38 (2009) 1477; (b) Y.S. Li, F.Y. Liang, H. Bux, A. Feldhoff, W.S. Yang, J. Caro, *Angew. Chem.* 122 (2010) 558.
- [6] (a) H. Jung, A. Dubey, H.J. Koo, V. Vajpayee, T.R. Cook, H. Kim, S.C. Kang, P.J. Stang, K.W. Chi, *Chem. Eur. J.* 19 (2013) 6709; (b) H. Miyasaka, *Acc. Chem. Res.* 46 (2013) 248; (c) M.L. Hu, A. Morsali, L. Aboutorabi, *Coord. Chem. Rev.* 255 (2011) 2821.
- [7] (a) M. Kandiah, M.H. Nilsen, S. Usseglio, S. Jakobsen, U. Olsbye, M. Tilset, C. Larabi, E.A. Quadrelli, F. Bonino, K.P. Lillerud, *Chem. Mater.* 22 (2010) 6632; (b) L. Valenzano, B. Civalleri, S. Chavan, S. Bordiga, M.H. Nilsen, S. Jakobsen, K.P. Lillerud, C. Lamberti, *Chem. Mater.* 23 (2011) 1700.
- [8] (a) S. Biswas, P. Van der Voort, *Eur. J. Inorg. Chem.* 12 (2013) 2154; (b) A. Schaate, P. Roy, A. Godt, J. Lippke, F. Waltz, M. Wiebecke, P. Behrens, *Chem. Eur. J.* 17 (2011) 6643.
- [9] A.K. Cheetham, C.N.R. Rao, R.K. Feller, *Chem. Commun.* 46 (2006) 4780.
- [10] (a) Y.S. Zhang, S.R. Breeze, S.I. Wang, J.E. Greedan, N.P. Raju, L.J. Li, *Can. J. Chem.* 77 (1999) 1424; (b) Y.F. Han, Y. Fei, G.X. Jin, *Dalton Trans.* 39 (2010) 3976; (c) A.D. Burrows, K. Cassar, M.F. Mahon, S.P. Rigby, J.E. Warren, *CrystEngComm* 10 (2008) 1474; (d) H. Sato, R. Takase, Y. Mori, A. Yamagishi, *Dalton Trans.* 41 (2012) 47.
- [11] G.I. Spijksma, H.J.M. Bouwmeester, D.H.A. Blank, A. Fischer, M. Henry, V.G. Kessler, *Inorg. Chem.* 44 (2006) 4938.
- [12] (a) J.L. Hoard, J.V. Silverton, *Inorg. Chem.* 2 (1963) 235; (b) B. Allard, *J. Nucl. Inorg. Chem.* 43 (1987) 789; (c) W. Clegg, *Acta Crystallogr., Sect. C* 43 (1987) 789–791; (d) S.C. Chaudhry, C. Verma, S.S. Bhatt, N. Sharma, *Ind. J. Chem. Sect. A* 47 (2008) 43; (e) Zherikova, *Zh. Strukt. Khim.* 46 (2005) 1081.
- [13] (a) F.A. Cotton, R.C. Elder, *Inorg. Chem.* 4 (1965) 1145; (b) M.J. Bennett, F.A. Cotton, R. Eiss, *Acta Crystallogr., Sect. B* 24 (1968) 904; (c) Z.A. Starikova, E.A. Shugam, *Zh. Strukt. Khim.* 10 (1969) 267.
- [14] J.D. Watson, F.H.C. Crick, *Nature* 171 (1953) 737.
- [15] Y.H. Hu, L. Zhang, *Adv. Mater.* 22 (2010) E117.
- [16] A. Thompson, D. Attwood, E. Gullikson, M. Howells, K.J. Kim, J. Kirz, J. Kortright, I. Lindau, P. Pianatta, A. Robinson, J. Scofield, J. Underwood, D. Vaughan, G. Williams, H. Winick, *X-ray Data Booklet*, Berkeley, California 94720, 2001.
- [17] G.N. George, I.J. Pickering, *EXAFSPAK – A Suite of Computer Programs for Analysis of X-ray Absorption Spectra*, SSRL, Stanford, CA, 1993.
- [18] S.I. Zabinsky, J.J. Rehr, A. Ankudinov, R.C. Albers, M.J. Eller, *Phys. Rev. B* 52 (1995) 2995.